Multimed Tools Appl (2019) 78:12917–12937
https://doi.org/10.1007/s11042-018-6421-7

A hybrid edge-based technique for segmentation of renal lesions in CT images

Ravinder Kaur[1] · **Mamta Juneja**[1] · **A. K. Mandal**[2]

Received: 19 September 2017 / Revised: 13 July 2018 / Accepted: 15 July 2018 /
Published online: 1 August 2018

Abstract The entire community of medical experts uses various imaging techniques as the precursor for disease diagnosis with the assistance of computer-aided diagnosis systems. In many cases, these imaging techniques savored the status of pivotal proof of occurrence for tissue abnormalities. One of the most important steps in the analysis of tissue using medical images is the correct approximation of position, size, and shape of the lesion which plays a significant role to decrease false positives count for effective diagnosis of renal lesions. This article suggests a hybrid segmentation technique based on two methods which include spatial intuitionistic fuzzy c-means clustering (SIFCM) that integrates spatial image details and, distance regularized level-sets method for extraction of renal lesions correctly and proficiently in computed tomography (CT) images. The proposed technique works by taking an approximation of region of interest (ROI) given by Spatial IFCM clustering (SIFCM) for correct demarcation of lesions. Further, the performance of the suggested technique is tested on the considered image dataset and compared with the other state-of-the-art segmentation techniques such as thresholding, region growing, level set, fuzzy c-means clustering (FCM), active contour without edges (ACWE), geodesic active contours (GAC), spatial FCM and intuitionistic FCM. To confirm the segmentation results, the ground truth marked by the expert radiologists was considered as a gold standard for comparison. The experimental outcomes reveal that the suggested technique yields the results close to the manual delineations of experts as compared to the other considered segmentation techniques and is able to segment

✉ Ravinder Kaur
ravinder.kaur7@yahoo.com

Mamta Juneja
mamtajuneja@pu.ac.in

A. K. Mandal
drarupkumar@gmail.com

[1] UIET, Panjab University, Chandigarh, India

[2] PGIMER, Chandigarh, India

lesion correctly and precisely. The suggested technique attains the better lesion segmentation, even for images with low-contrast and in the presence of noise components. Furthermore, it possesses the capability to control the parameters adaptively from SIFCM clustering method.

Keywords Renal lesion · Segmentation · Spatial FCM · IFCM · GAC · DRLSE · CT images

1 Introduction

Renal cancer is one of the prominent causes of increase in mortality rates around the globe. According to the American cancer society (ACS), the estimated number of new renal cancer cases and deaths are 63,990 and 14,400 respectively, as reported in 2016 [25]. The premature diagnosis is essential and important for the correct treatment of renal cancer [26, 30]. Hence, it is imperative to effectively segment and classify the renal lesions due to aggressive nature of certain types of renal lesions and rapid drop in survival rates with the disease advancement [2, 3, 15]. Moreover, the success of radiotherapy (RT) relies on precise segmentation of target tissue and minimum dose to the tissues adjacent to the abnormal target tissue. Thus, it is essential to have knowledge about the precise shape and essential boundaries of the abnormal tissues at peril while planning the treatment, in order to attain adequate tumor control and to evade later detrimental consequences. CT is considered as the gold standard among all the available imaging modalities for work up with renal lesions, and initial detection of lesions using CT images is well described in several articles and books [4, 6, 9, 14, 16, 22]. CT image is suitable to detect renal lesion as it provides high-resolution images with good anatomical details and it may contain distorted components due to artifacts, which include noise, ring, scatter, motion, beam hardening, pseudo-enhancement, metal, and helical artifacts, etc. Hence, segmentation of renal lesion from a given CT image is an essential and challenging task due to the presence of noise components or for images with low contrast. In medical imaging, different techniques have been proposed and validated on diverse applications. In spite of much technical advancement, the researchers or practitioners are still facing the problem of identifying that which technique is suitable for a specific segmentation problem. One of the key challenges in the segmentation is to accurately delineate the boundary of renal lesion among nearby tissues due to the presence of intrinsic intensity in-homogeneity of tissue texture or boundaries that are inherently fuzzy which makes the task of segmentation more difficult.

Segmentation is usually performed after preprocessing for accurate delineation of renal lesions from CT images to perform analysis on segmented tissue or pathological regions. The accuracy of segmentation technique plays a crucial role in classifying the lesions as benign or malignant because the shape and texture features rely on the boundary of the extracted lesion. In literature, different techniques have been proposed for delineation of renal lesions in CT images such as region growing [17], thresholding [27], clustering [24], geodesic active contour, level sets [21] and many others. An attempt to segment renal lesion from CT images was made by Kim et al. [17] who proposed a computerized system for segmentation of renal tumors from CT images. Based on texture analysis, a seed point was selected within the tumor region and the region-growing algorithm was employed for segmentation. The drawback of using a region growing technique is that it suffers from over and under-segmentation which makes it less suitable for such applications. Summers et al. [27] made another attempt where they proposed a thresholding based approach for segmentation of renal lesions, but the limitation of the technique was that its accuracy relies on the chosen threshold value. Further,

Piao et al. [24] employed fuzzy c-means and level set method to segment lesion from CT images. Linguraru et al. [21] employed fast marching technique followed by geodesic active contour level sets for segmentation of renal lesions. Lee et al. [18] utilized region growing and active contours for segmentation of small renal masses from contrast-enhanced CT images. Presently, deformable models have gained the attention of different researchers for medical image segmentation which includes the snakes, active contour model, level sets, etc. However, the snake and level sets are the two main approaches which are employed for the execution of active contour, that rely on energy function optimization. But the problem with the snake technique is that it requires initial contour and converges poorly in the presence of noise as the curve propagates unambiguously on defined snake points [7, 18]. Contrary, Osher, and Sethian [23] suggested a level set method which has proven to be efficient to address the issue of medical image segmentation as it depends on the partial differential equations (PDE) for implicit curve propagation by progressing the level set function (LSF) rather than moving the contours. However, in some cases zero LSF moves away from the probable boundary and to solve this issue, Li et al. [19] presented a geodesic active contour (GAC) method that utilizes image intensity features to control the contour evolution, and it has been used by researchers for segmentation. A limitation of GAC is that scientific knowledge is necessary for setting the parameter values and it requires tedious manual interference. GAC works on the assumption of homogeneity in the region of interest (ROI) and nearby regions, but this supposition is disrupted in medical CT images because of the presence of intensity inhomogeneity in the texture of the surrounding tissues. Further, the distance regularized level set evolution method (DRLSE) was introduced with a novel distance regularization metric given by external energy and potential functions for effective curve propagation, and it works by eliminating the undesirable effects announced by the LSF. However, the effectiveness of the level set technique mainly relies on the correct initialization of contour and selection of suitable parameter values employed for level set contour propagation. Also, it requires the manual interference which makes it a labor-intensive, time-consuming and knowledge dependent. The main limitations of existing segmentation techniques are that they require human interactions such as for determining initial contours or the pre-marked ROIs. Additionally, recreating and training the techniques is also tedious, particularly for images which possess complex details.

Recently, fuzzy based techniques using spatial constraints are attracting different researchers to address medical image segmentation difficulties [1, 5, 8, 10, 12, 28, 29]. As per reviewed literature, no research work was found on spatial intuitionistic FCM (SIFCM) clustering and distance regularized level set method for segmentation of renal lesions in CT images. In this research article, a hybrid technique is proposed by combining features of spatial intuitionistic fuzzy c-means (SIFCM) clustering, and distance regularized level set evolution (DRLSE) for segmentation of renal lesions in CT images. Initially, it starts with SIFCM clustering which incorporates image spatial information followed by DRLSE whose parameters are directly obtained from SIFCM to extract the lesion from a given CT image. The suggested technique is tested and validated on CT image dataset used in this study, by comparing its outcomes against ground truth generated by domain experts. Due to unavailability of the standard dataset, the dataset of renal lesion CT images have been acquired from the hospital and is employed to compare and analyze the performance of various segmentation techniques using considered evaluation metrics.

The rest of the article is organized as follows: The background of SIFCM clustering and the DRLSE segmentation methods is given in Section 2. In Section 3, the experimental results are discussed and compared with the existing techniques. Section 4 covers the brief discussion on the gathered results. Lastly, the conclusion is given in Section 5.

2 Methods

2.1 Spatial intuitionistic fuzzy C-means clustering (SIFCM)

In recent years, clustering based segmentation approaches are prevalent for the segmentation of abnormal image regions due to the presence of fuzziness in medical images. Fuzzy c-means (FCM) clustering method is among the most prevalent methods in the domain of fuzzy clustering which has been extensively used to analyze different medical images [5, 10]. The FCM was proposed to address the limitations of K-means clustering where every pixel value can only be assigned to one of the K clusters. Contrary, FCM employs a membership function μ_{jk} to express the degree of membership of the *kth* object to the *jth* cluster and is beneficial for delineation of abnormal tissues in different types of medical images because of intensity inhomogeneities. In FCM clustering, similar pixel values are grouped together to form one cluster repetitively by decreasing the value of cost function that relies on the Euclidean distance between the pixel value and cluster centers of the diverse clusters. The problem with the FCM is that it does not consider the uncertainty arises during specifying the membership function and its accuracy is affected by the presence of noise which mimics the characteristics of the tissue. Further, to address the shortcomings of FCM, intuitionistic fuzzy c-means (IFCM) clustering was suggested to incorporate the additional uncertainty in terms of hesitation degree that originates, because of inadequate knowledge while specifying the membership function. IFCM has shown better results in the segmentation of medical images, but its performance may be affected in the presence of noise as spatial details of image pixels are not incorporated. Consequently, to address the issues of the IFCM segmentation method, the authors have suggested the spatial intuitionistic fuzzy c-means clustering (SIFCM) which uses a new cost function by incorporating spatial details of the image for segmentation of renal lesions in CT images. The objective function in conventional FCM is given as:

$$F_M(U, v, \chi) = \sum_{l=1}^{C} \sum_{m=1}^{N} (u_{lm})^M D^2(x_m, v_l) \tag{1}$$

Here $D(x_m, v_l)$ denotes Euclidean distance between cluster center or centroid, v_l and x_m, u_{lm} denotes the membership value of m^{th} data point in l^{th} cluster. N is pixels count of the image under consideration and C represents cluster count. Thus, by minimizing the objective function F_M, the values of cluster center or centroids and membership functions and are amended repetitively using the mathematical expressions given below:

$$u_{lm} = \frac{1}{\sum_{n=1}^{C} \left[D_{lm}^2 \Big/ D_{nm}^2 \right]^{1/M-1}} \tag{2}$$

$$v_l = \frac{\sum_{m=1}^{N} \mu_{lm}^M \chi_m}{\sum_{m=1}^{N} \mu_{lm}^M} \tag{3}$$

Fuzzy set considers only membership function u_{lm} but an intuitionistic fuzzy set examines both membership $u_{lm}(x)$ and non-membership function $N(x) = 1 - u_{lm}(x)$, where $x \epsilon [0,1]$. The intuitionistic fuzzy set A in X and the hesitation degree is given as:

$$A = \left\{ x, \quad \mu_A(x), \quad (1-\mu_A(x)^{\alpha})^{1/\alpha} \quad | \, x \epsilon X, \alpha > 0 \right\} \tag{4}$$

$$\Pi_A(x) = 1 - \mu_A(x) - (1-\mu_A(x)^{\alpha})^{1/\alpha} \tag{5}$$

The Eq. (5) can be used to calculate the hesitation degree and the membership function (μ^*_{lm}) for IFCM method is given as:

$$\mu^*_{lm} = u_{lm} + \pi_{lm} \tag{6}$$

The value of cluster center for IFCM is calculated as:

$$v^*_l = \frac{\sum_{m=1}^{N} \mu^*_{lm} \chi_m}{\sum_{m=1}^{N} \mu^*_{lm}} \tag{7}$$

The values of the cluster center and the membership function are amended at every iteration, and the method terminates when the termination condition is satisfied i.e. $max_{l,m} \left| \mu^{*new}_{lm} - \mu^{*previous}_{lm} \right| < \epsilon$, where ϵ is value defined by user, a a $\epsilon = 0.03$.

In IFCM clustering method, the cluster centers and the membership function are adaptively estimated to minimize the value of cost function. However, the adjoining pixels in medical images are inter-related to each other because of similar features, and there is a high possibility of two different pixel values to fall in the same cluster [10]. Thus, spatial relationship among the pixel values plays a significant role in IFCM. Consequently, the authors of this paper have made an attempt to suggest a new membership function by integrating the spatial information into the membership function of IFCM for correct segmentation of renal lesions, and the method is named as SIFCM. The suggested SIFCM clustering method for the evolution of level set function is presented as Method 1.

Method 1: Spatial Intuitionistic Fuzzy C-Means clustering (SIFCM)

Input: Image **Output:** Segmented image

Step 1: Initialize ϵ,number of clusters C, membership parameter 'M,' and fuzzy membership matrix $U = u_{lm}$, where l is the pixel index, m is the cluster index.

Step 2: Calculate the value of cluster centers or centroids by employing Eq. (7) and the objective function F_M using Eq. (1).

Step 3: Update the membership matrix values as discussed above using

$$u_{lm} = \frac{1}{\sum_{n=1}^{C} \left[D^2_{lm} / D^2_{nm} \right]^{1/M-1}} \tag{8}$$

$$\mu^*_{lm} = u_{lm} + \pi_{lm} \tag{9}$$

Step 4: Integrate spatial information using h_{lm}^{z}, which is calculated as:

$$h_{lm}^{z} = \sum_{k \in N_n} \mu_{mk}^{*} \tag{10}$$

Here, N_n indicates a local window frame fixed around the pixel value 'n' in a fuzzy spatial domain.

Step 5: Calculate new membership function by incorporating h_{lm}^{z} in the previous membership function

$$\mu_{lm}^{*Snew} = \frac{\mu_{lm}^{*w} h_{lm}^{z}}{\sum_{y=1}^{C} \mu_{ym}^{*w} h_{ym}^{z}} \tag{11}$$

Here w and z are two parameters which control the respective contribution to determine the relative weightage of the initial membership (M) and the spatial function respectively. Based on the experimental analysis, in this work, the value of w and z is taken as 1.

Step 6: If the condition $max_{l,m} \left| \mu_{lm}^{*Snew} - \mu_{lm}^{*Sprevious} \right| < \in$ satisfies then terminate the loop, else go to step 2.

The SIFCM clustering method consists of two phases. Initially, it determines the values of membership function by computing the Euclidean distance between pixel values and cluster centers or centroids. Then, the obtained membership value is employed in the spatial domain to obtain the new spatial membership function. The considered variable in the spatial domain h_{lm}^{z}, strengthens the membership function and the process of SIFCM continues in an iterative manner with the new membership function obtained by including spatial details of imathe ge. This repetitive procedure is terminated if the variation among the two consecutive cluster centers or centroids is below $\in$.

2.2 Distance regularized level set evolution (DRLSE)

The deformable model based level set method is extensively employed to address the issue of vital disparity edges for segmentation in CT images. Initially, the segmentation model based on level set method was suggested by Osher and Sethian for the evolution of contours [23]. The primary problem with the conventional level set technique is the contour re-initialization to ensure correct results at the rate of excessive computation cost. In order to address this limitation, Li et al. suggested distance regularized level set evolution (DRLSE) by integrating new distance regularized term with energy and two potential functions in the conventional level set method. DRLSE not only addressed the problem of re-initialization but it also lessens the computational complexity. Thus, the DRLSE is defined as follows:

$$Eg(\gamma) = \mu Reg(\gamma) + Eg_{ext}(\gamma) \tag{12}$$

Where, $Eg(\gamma)$ represents the energy function which consist of $Reg(\gamma)$, regularization term that forces γ to automatically proceed towards the signed distance function throughout the LSF progression, and external energy $Eg_{ext}(\gamma)$ which forces the accurate evolution of contour in the desired direction and is given as:

$$Eg_{ext} = \lambda l(\gamma) + \alpha Ar(\gamma) \tag{13}$$

The parameter $\mu > 0$, denotes the regularization term coefficient. The value of cthe oefficient of contour length, λ should be greater than zero in order to regulate the contour smoothness during evolution and α, is another coefficient whose value can either be negative or positive depending upon the initial contour position. Further, the terms in the external energy function, Eg_{ext} are defined as follows:

$$l(\gamma) \triangleq \int_{\Omega} e\delta_{\epsilon pi}(\gamma)|\nabla\gamma|dx \tag{14}$$

$$Ar(\gamma) \triangleq \int_{\Omega} eh_e(-\gamma)dx \tag{15}$$

Here, e represents the edge indicator functions, $\delta_{\epsilon pi}(x)$ is Dirac delta function and $h_e(x)$ denotes the heaviside function. The values for these functions can be calculated as:

$$e \triangleq \frac{1}{1 + |\nabla g_{\sigma} * Img|^2} \tag{16}$$

$$\delta_{\epsilon pi}(x) = \begin{cases} 0, & |x| > \epsilon pi \\ \dfrac{1}{2\epsilon pi\left[1 + \cos\left(\dfrac{\pi x}{\epsilon pi}\right)\right]}, & |x| \leq \epsilon pi \end{cases} \tag{17}$$

$$h_e(x) = \begin{cases} 0, & x < -\epsilon pi \\ 1, & x > \epsilon pi \\ \dfrac{1}{2}\left[1 + \dfrac{x}{\epsilon pi} + \dfrac{1}{\pi}\sin\left(\dfrac{\pi x}{\epsilon pi}\right)\right], & |x| \leq \epsilon pi \end{cases} \tag{18}$$

Here, the original image is denoted by Img and e is the image obtained by performing convolution on original image with the Gaussian kernel (g_{σ}), where (σ) denotes the standard deviation. ϵpi is a constant metric to control the regularization of the Dirac delta function, in this scenario the value of $\epsilon pi = 1.5$. $Reg(\gamma)$, indicates the regularization term for level set meta hod which is calculated as:

$$Reg(\gamma) \triangleq \int_{\Omega} \rho(|\nabla\gamma|)dx \tag{19}$$

The potential function for the regularized term $Reg(\gamma)$ is denoted by $\rho(|\nabla\gamma|$ and a double well potential function is expressed as:

$$\rho(y) = \begin{cases} \dfrac{1}{2}(y-1)^2, & y \geq 1 \\ \dfrac{1}{4\pi^2}(1-\cos(2\pi y)), & y \leq 1 \end{cases} \tag{20}$$

By computing the first derivative, the above equation can be written as:

$$\rho'(y) = \begin{cases} (y-1), & y \geq 1 \\ \dfrac{\sin(2\pi y)}{2\pi}, & y \leq 1 \end{cases} \tag{21}$$

Hence the total energy function can be expressed as:

$$Eg(\gamma) = \mu \int_{\Omega} \rho(|\nabla\gamma|)dx + \lambda \int_{\Omega} e\delta_{epi}(\gamma)|\nabla\gamma|dx + \alpha \int_{\Omega} eh_e(-\gamma)dx \tag{22}$$

The total energy is further decreased by calculating the gradient flow, which is specified as follows:

$$\frac{\partial\gamma}{\partial t} = \mu\, div\left[\left(\frac{\rho'(|\nabla\gamma|)}{|\nabla\gamma|}\right)\nabla\gamma\right] + \lambda\delta_{epi}(\gamma)\, div\left[e\frac{\nabla\gamma}{|\nabla\gamma|}\right] + \alpha e\delta_{epi}(\gamma) \tag{23}$$

The Eq. 23 represents the edge based active contour model with distance regularization level set formulation. The first term on the right side of Eq. 23 denotes the distance regularization energy whereas the gradient flow of the different energy function is specified by second and third terms as given in Eq. 14 and Eq. 15. However in DRLSE, the initial formulation of level set function $\gamma_0(i,j)$ is given as:

$$\gamma_0(i,j) = \begin{cases} -b_0, & (i,j) < \Omega_0 \\ b_0, & otherwise \end{cases} \tag{24}$$

Here, $b_0 > 2$ ϵpi is a constant metric and Ω_0 is ROI in the considered image. Further, the discretization of Eq. (23) is further expressed as:

$$\gamma_{t+1}(i,j) = \gamma_t(i,j) + \tau\frac{\partial\gamma_{t(i,j)}}{\partial t} \tag{25}$$

Where τ represent the time step for the evolution of level set.

2.3 Proposed technique (hybrid of SIFCM and DRLSE)

In the proposed technique, the SIFCM clustering scheme and the edge based distance regularized level set evolution method is employed for segmentation of renal lesions in CT images. The proposed technique consists of two steps: initially, the SIFCM clustering scheme is implemented which utilizes hesitation degree and spatial details of the image to roughly estimate the shape of the lesion in a given CT image. For SIFCM clustering, the values of the parameters w and z as taken as 1 and the iteration is terminated when the difference between the two clusters centers at two successive iterations is less than a threshold which is $\in$ =0.03. Further, a 3×3 window size is used throughout this work. Consecutively, the outcomes of the SIFCM scheme are given as input to DRLSE for initialization and regularization of the level set method by approximating the variable parameters such as τ, α, μ, λ *and* εpi. The correct result of segmentation technique relies on preliminary shape and position of level set function, therefore, proper initialization of level set function near the boundary of lesion is the essential for the correct demarcation.

Suppose the outcome of the SIFCM technique is denoted by I_R and the corresponding membership function is denoted as μ_m^{SIFCM}. The initial level set function can be expressed as:

$$\gamma_0(i,j) = (4I_R - 2)\,\varepsilon pi \tag{26}$$

Where, $\varepsilon pi = 1.5$ is taken in curthe rent study [20] which helps to regulate the Dirac delta function [11, 19, 20] and I_R represent the binary image attained by the thresholding with the given threshold value (Th), $0 < \mathrm{Th} < 1$, as:

$$I_R = \begin{cases} 0, & \mu_m^{SIFCM} < Th \\ 1, & \mu_m^{SIFCM} > Th \end{cases} \tag{27}$$

Further, there are numerous parameters associated with DRLSE which are responsible for correct segmentation of lesions from a given CT image. Hence, it is essential to adjust them to obtain correct segmentation outcomes by following some rules, for their optimal configuration. The higher value of σ, performs over-smoothing of the image by eliminating important image details. The sign with balloon force (α), affects the direction of level set curve propagation such as if the preliminary level set function (γ) is exterior to the ROI then it is necessary to keep a sign of α as positive for contraction, and vice versa. The large values of τ, time step parameter, may speed up the contour propagation of DRLSE at the cost of boundary leakages. The mentioned rules, however effective, are inadequate for deciding the values of parameters for a given CT image. Thus, it is required to adjust these guiding parameters by SIFCM. The balloon force (α) must be high, and it is determined by its sign which can be positive (to contract in the direction of the lesion borders) or negative (to grow in the direction of the lesion borders). The balloon force is calculated as:

$$\alpha = 2\left(\mu_m^{SIFCM} - 0.5\right) \tag{28}$$

The outcome of SIFCM clustering is employed to form the initial level set function denoted by γ_0^{SIFCM}, and time step parameter 'τ' is for the DRLS progression is calculated by approximating the area and length of the preliminary level set function estimated as:

$$\tau = \frac{\int_\Omega h_e(\gamma_0(i,j))dx\,dy}{\int_\Omega \delta_{\epsilon pi}(\gamma_0(i,j))dx\,dy} \tag{29}$$

Depending on investigational outcomes, the weighting coefficient of the curve length (λ) and distance regularization term (μ) is defined as:

$$\lambda = 0.1 * \tau \tag{30}$$

$$\mu = \frac{0.2}{\tau} \tag{31}$$

The issue of boundary leakages can be avoided by controlling λ and, for accurate and stable contour propagation the product of τ and μ must be less than 1/4 [20, 23]. Thus, implement the progressing equation for level set function as:

$$\frac{\partial \gamma}{\partial t} = \mu\, div\left[\left(\frac{\rho'(|\nabla\gamma|)}{|\nabla\gamma|}\right)\nabla\gamma\right] + \lambda\delta_{\epsilon pi}(\gamma)\, div\left[e\frac{\nabla\gamma}{|\nabla\gamma|}\right] + 2e\left(\mu_m^{SIFCM} - 0.5\right)\delta_{\epsilon pi}(\gamma) \tag{32}$$

The proposed technique works in a semi-automatic manner after one time initialization of required parameters, which further do not require any human interference. This improvement leads to a new technique for segmentation of renal lesion in CT image with many benefits. With the help of such improvement, one can avoid unnecessary or inadequate segmentation results which are produced if human interference is involved.

3 Experimental results

3.1 Image dataset

Due to unavailability of the standard dataset on renal CT images, different techniques proposed in the literature were tested and validated on dataset acquired by authors from different hospitals. In this research study, contrast-enhanced renal CT scans of 40 subjects were gathered from the department of Radio-diagnosis, post graduate institute of medical education and research (PGIMER), Chandigarh, India. The dataset consists of benign and malignant renal lesions. The size of images is 512 × 512 pixels that were captured with a 12-bit depth using 128 slice SIEMENS CT scanner. The boundary of each lesion was marked by expert radiologists, and this manual delineation was taken as the ground truth for carrying out the comparative analysis. The proposed technique was implemented and tested in Matlab 2016b environment on Dell 2.00-GHz Dual-core Laptop.

3.2 Performance assessment parameters

The performance of the suggested segmentation technique for renal lesions has been validated using the parameters based on area and boundaries of the extracted lesions. The metrics based on area and boundaries of the segmented lesion are employed to convey the number of correct or incorrect pixels enclosed by the proposed technique. The parameters considered to quantitatively analyze the performance of the proposed technique are discussed in this section [13]:

a) **True Positive rate (TP) or Sensitivity or Recall:** True positive represents the proportion of pixel values that are considered as a lesion in the binary masks of both the manual segmentation and computer segmentation technique. A higher value of true positives indicates that the outcome of the segmentation technique is close to ground truth marked by the expert.

$$TP = \frac{TP}{TP + FN} \times 100 \tag{33}$$

b) **False positive rate (FP):** False positive represents the proportion of pixel values that are considered as lesion by the computer segmentation technique but not in ground truth.

$$FP = \frac{FP}{FP + TN} \times 100 \tag{34}$$

The lower value of FP means less incorrect pixel values are covered by the computerized segmentation technique.

c) **True negative rate (TN):** True negative, represents the proportion of pixel values that are considered as normal tissue in the binary masks of both the manual segmentation and computer segmentation technique. A higher value of true negative rate indicates the better performance of segmentation technique.

$$TN = (1 - FP) \times 100 \tag{35}$$

d) **Accuracy (ACC):** Accuracy is used to measure the fraction of pixel values present in the computerized segmented lesion out of all the pixel values in manual demarcation. It is defined as:

$$ACC = \frac{TP + TN}{TP + FP + TN + FN} \tag{36}$$

Where FP, FN, TN, TP denotes false positive, false negative, true negative and true positive respectively.

e) **Jaccard index (JI):** It is utilized to measure statistical resemblance among the areas segmented by the computerized technique and manual delineations. The higher value of JI signifies good match among regions obtained by the computerized technique and manual segmentation. JI is calculated as:

$$JI = \frac{|S_m \cap S_a|}{|S_m \cup S_a|} \tag{37}$$

Where S_m represents the binary mask of the manual segmentation generated by the domain experts and S_a represents the binary mask generated by the proposed technique.

f) **Dice similarity coefficient (DC):** Dice similarity coefficient can also be employed to find the correspondence among the segmentation results of the proposed technique and manually delineation given by the experts. The value of DC must be near to unity in order to ensure the correct match between the manually delineated region and the segmented outcome. DC is expressed as:

$$DC = 2 \times \frac{|S_m \cap S_a|}{|S_m + S_a|} \tag{38}$$

g) **Hausdorff distance (HD):** It measures the structural differences among two given objects and is the minimum distance between the ground truth and segmented region. Suppose, $S_m = \{s_{m1}s_{m2}, \ldots . s_{mi}\}$ be the curve generated by manually the marked ground truth of the lesion and $S_a = \{s_{a1}s_{a2}, \ldots . s_{ai}\}$ is the curve formed by computerized methothe d. Then the hausdorff distance from S_m to S_a is given as:

$$HD(S_m, S_a) = max(h(S_m, S_a), h(S_a, S_m)) \tag{39}$$

Where $h(S_m, S_a) = \max_{s_m \in S_m} \min_{s_a \in S_A} \|s_m - s_a\|$. The lower value of HD indicates better segmentation results.

3.3 Comparison of SIFCM clustering method with the other segmentation techniques

In order to evaluate the performance of the SIFCM clustering method, various CT images have been taken, one of them is displayed in Fig. 1(a).The outcomes of the SIFCM have been compared with other segmentation approaches such as thresholding, region growing, FCM [21], SFCM [10], and IFCM [11] using different performance evaluation parameters and also in terms of computation time as mentioned in Table 1.

From the results given in Table 1, it can be observed that the SIFCM method is capable to effectively segment the expected region of the interest. As revealed from Fig. 1(c) and (d), the results of thresholding and region growing technique are not convincing as they require an ideal threshold value that varies for different kind of images, especially for the boundaries which are merged with the adjoining tissues. Moreover, the FCM is unable to correctly segment the lesion because of large contrast disparities in image regions and fused fragile boundaries as presented in Fig. 1(e), which results to over-segmentation. The performance of FCM degrades in the presence of noise artifacts which results to the improper classification of uncertain pixels into the foreground. In contrast, the output of spatial FCM (SFCM) and intuitionistic FCM (IFCM) has improved the results of traditional FCM technique by incorporating spatial constraints and hesitation degree respectively. However, the result of spatial FCM is affected in the presence of weak and uncertain boundaries of the lesion. The uneven and weak edges of renal lesion often complicate the segmentation process due to the presence of intensity inhomogeneities. Figure 1(h) illustrates comparatively actual and correct segmentation of renal lesion. The lesion extracted by SIFCM clustering method is not leaked to the neighboring background regions, and consequently, lesion margin is comparatively clear. The segmentation results in terms of true positives, false positives, true negatives, accuracy, Jaccard index, dice similarity coefficient (DC) and Hausdorff distance obtained by proposed SIFCM methods and other segmentation techniques are given in Table 1 which illustrates that the SIFCM method converges to higher values as compared to the other aforementioned techniques.

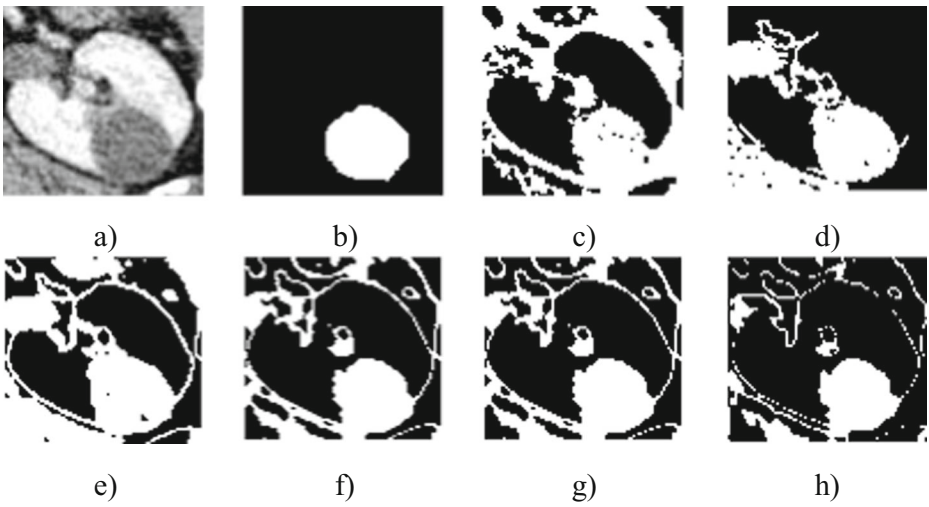

Fig. 1 Segmentation results of different techniques **a**) Original image containing renal lesion **b**) Ground truth of original image **c**) Thresholding **d**) Region Growing **e**) FCM **f**) SFCM **g**) IFCM **h**) Method1 (SIFCM)

Table 1 Comparative analysis of SIFCM method with considered segmentation algorithms

Techniques	Performance metrics							
	True positive rate or Recall (%)	False positive rate (%)	Accuracy (%)	Jaccard similarity	Dice coefficient	True negative rate (%)	Hausdorff distance	Time (s)
Thresholding	61.71 ± 8.5	12.16 ± 7.3	74.12 ± 26.3	0.682 ± 0.039	0.662 ± 0.023	87.84 ± 0.039	30.28 ± 0.28	0.89
Region Growing	71.47 ± 4.9	28.07 ± 22.6	78.42 ± 22.8	0.751 ± 0.032	0.701 ± 0.021	71.93 ± 0.164	25.08 ± 0.23	1.56
FCM	73.15 ± 4.3	27.07 ± 19.6	80.02 ± 28.4	0.761 ± 0.035	0.727 ± 0.028	72.93 ± 0.73	29.08 ± 0.25	5.78
SFCM	75.07 ± 3.9	25.23 ± 17.8	83.17 ± 26.3	0.774 ± 0.028	0.717 ± 0.032	74.77 ± 0.541	27.48 ± 0.22	5.87
IFCM	76.07 ± 5.3	24.13 ± 14.8	83.37 ± 25.2	0.772 ± 0.025	0.720 ± 0.027	75.87 ± 0.019	27.58 ± 0.20	5.83
Method 1 (SIFCM)	81.07 ± 3.1	12.02 ± 5.8	85.57 ± 19.2	0.801 ± 0.015	0.790 ± 0.024	87.98 ± 0.024	22.28 ± 0.18	5.99

3.4 Comparison of the proposed technique (a hybrid technique based on SIFCM and DRLSE) with the other segmentation techniques

The assessment of proposed hybrid technique based on SIFCM clustering and DRLS with other considered segmentation approaches such as active contour without edges (ACWE) [4], geodesic active contours (GAC), DRLSE [8] and fuzzy level set method (FLSM) [29] have been evaluated. The considered performance evaluation parameters and computation time on dataset are mentioned in Table 2. The higher value of TP and TN indicate that the proposed technique performs better extraction of the renal lesion by covering more area as compared to the other methods. From Table 2, it can be perceived that the suggested technique takes less execution time when compared with other discussed methods. It also possesses less value of HD, that measures the distance among the worst points in the given two contours, which signifies that the delineations made by the proposed technique are quite similar to the manual segmentation outlines marked by the experts. The qualitative results of considered segmentation methods are demonstrated in Fig. 2 where the initial contours are symbolized with white dashed lines. The ACWE, GAC and DRLSE segmentation methods require manual initialization to get the initial contour of the lesion for further segmentation task. However, these methods generated the even contour but did not provide accurate demarcation of lesion boundary due to the presence of noise or intensity in-homogeneity as shown in Fig. 1(c, d, f). Further, the ACWE and GAC delineate the lesion boundary, but they are unable to handle the real boundaries which result in boundary leakage into the nearby tissues as shown in Fig. 2(c, d). The FLSM wrongly classifies some of the uncertain pixel values into foreground region (Fig. 2(e)). The distance regularized level set method also leads to boundary leakage and is unable to generate the smooth contour even for the circular lesion (Fig. 2(f)). On the contrary, the suggested hybrid technique has the capability to handle intensity inhomogeneity, and it avoids the boundary leakage into surrounding tissues by using spatial information (Fig. 2(g)).The outcomes of suggested technique illustrate that it generates better demarcation of lesions as compared to the other techniques and are close to the ground truth marked by the experts.

3.4.1 Calculation of adjustable variables

The variables employed in the implementation of SIFCM are determined by changing their values to find the appropriate value. The adjustable parameters in SIFCM clustering method are window size and membership computation parameter (M).

Calculation of window size for SIFCM The window size in SIFCM clustering method plays a crucial role and distinct values of window size are selected to examine the performance of the SIFCM method in terms of considered evaluation measures as mentioned in Table 3. The experimentations were performed by employing different window size such as 3, 5, 7 and 9 and the corresponding results are reported. The experiment results reveal that the use of 3 as a window size leads to better values for all the considered parameters.

Calculation of membership parameter 'M' The membership parameter M in SIFCM clustering method is utilized to calculate membership function and the trials were executed by employing distinct values of M such as 2, 3, 4 and 5 in order to identify suitable value. In this research work, the value of M is fixed as 2 and this has been revealed from the experiments that small deviation is observed by fluctuating the values of M as presented in Table 4.

Table 2 Comparative analysis of proposed technique (Hybrid technique based on SIFCM and DRLSE) with the other segmentation techniques

Techniques	Performance metrics							
	True positive rate or Recall (%)	False positive rate (%)	Accuracy (%)	Jaccard similarity	Dice coefficient	True negative rate (%)	Hausdroof distance	Time (s)
ACWE	63.5 ± 19.5	36.7 ± 8.2	71.47 ± 26.8	0.697 ± 0.31	0.682 ± 0.028	63.3 ± 11.1	35.48 ± 0.31	7.23
GAC	65.5 ± 17.2	33.4 ± 8.8	74.55 ± 24.8	0.701 ± 0.028	0.692 ± 0.026	66.6 ± 6.5	34.14 ± 0.29	7.12
FCMLS	71.5 ± 15.9	26.7 ± 9.2	76.45 ± 23.6	0.752 ± 0.026	0.741 ± 0.021	73.3 ± 5.9	29.05 ± 0.24	7.98
DRLSE	80.5 ± 9.9	14.7 ± 7.6	80.25 ± 19.3	0.791 ± 0.024	0.801 ± 0.018	85.3 ± 4.6	23.22 ± 0.18	10.85
Proposed Technique (PT)	86.5 ± 7.2	9.7 ± 5.4	86.51 ± 11.5	0.885 ± 0.019	0.882 ± 0.013	90.3 ± 4.2	20.45 ± 0.25	6.54

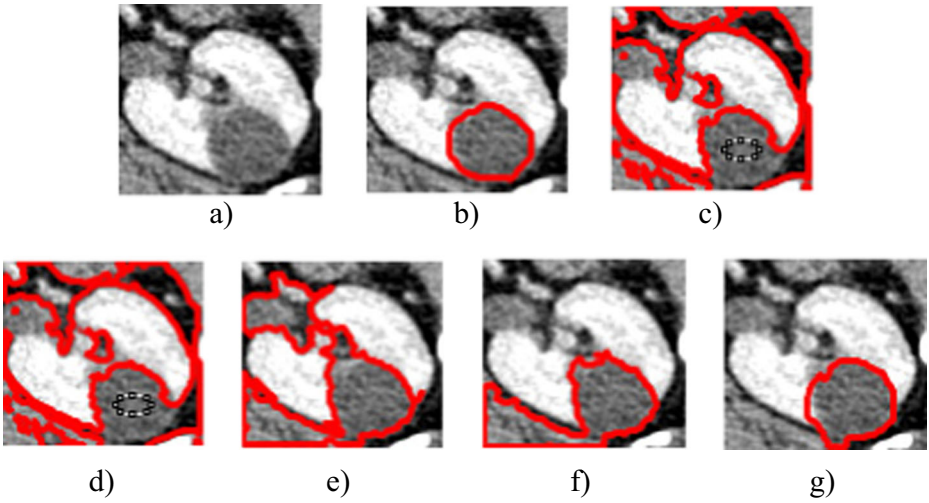

Fig. 2 Segmentation results of different techniques **a**) Original image containing renal lesion **b**) Ground truth of original image **c**) User initialized: active contour without edges with 250 iterations and initial contour marked as white dotted line **d**) GAC **e**) FLSM **f**) User initialized level set after 100 iterations **g**) Proposed technique after 20 iterations

4 Discussion

In this research study, a hybrid technique has been proposed for segmentation of renal lesion with the use of SIFCM clustering to initialize level set function without human interference. The suggested SIFCM clustering integrates the spatial details of the image with intuitionistic fuzzy clustering and is less susceptible to noise present in the image with the capability to attain probable lesion regions adaptively. Previously, all variations of level set methods suggested in the literature require the manual initialization which is subjected to human bias as they need expert knowledge and experience. Moreover, the user needs to be careful while dealing with the images containing weak or vague boundaries, to avoid over or inadequate segmentation results. In case of DRLSE, the value of α is determined according to the considered image but in case of the proposed technique, the value of α is calculated adaptively using the weighted area of the ROI predicted by the SIFCM clustering method. The proposed technique calculates the values of appropriate parameters automatically from outcomes of SIFCM clustering thus; SIFCM provides prior details to the DRLSE for its evolution. This can be observed from graphs given in Fig. 3 and the results discussed above that the proposed technique has attained less number of false positives which show its low ratio of incorrect segmentation. Moreover, it possesses the highest DC, JI, TP and TN values which signify that

Table 3 Performance of SIFCM method at distinct window sizes

Window size	True positive	False positive	Accuracy	Jaccard similarity	Dice coefficient	Hausdorff distance
3	86.50	9.7	85.71	0.885	0.882	20.45
5	85.86	8.9	84.89	0.877	0.878	21.19
7	85.75	8.6	84.78	0.875	0.872	21.75
9	85.64	8.4	84.67	0.871	0.871	21.84

Table 4 Performance of SIFCM method at distinct values of 'M'

Membership (M)	True positive	False positive	Accuracy	Jaccard similarity	Dice coefficient	Hausdorff distance
2	86.50	9.7	85.71	0.885	0.882	20.45
3	86.21	9.8	85.54	0.881	0.881	20.47
4	85.98	8.9	85.21	0.878	0.879	20.51
5	85.54	8.7	84.92	0.879	0.877	20.55

the lesion boundaries defined by the proposed technique are more accurate among all other discussed methods. Further, the similarity of the segmented lesions by the proposed technique with the ground truth image is validated by HD which illustrates that the suggested technique achieves the improved performance as compared to all other methods. From Fig. 1(a), this can be observed that the considered image has some noise components and vague edges, the FCM method for image segmentation is incapable to demarcate lesions precisely and it seepage out through weak edges to the surrounding tissues as shown in Fig. 1(e). On the other hand, the results of SFCM and IFCM are comparatively better and they are able to segment the lesion with less leakage to the nearby tissues due to their ability to incorporate spatial information and hesitation degree respectively as shown in Fig. 1(g) and (h). This has been revealed from the observed results that the SIFCM provides satisfactory results, which permits the separation among the lesion and nearby boundaries or small image features that simplify the delineation of lesion borders for the approximation of initial contour. Furthermore, the segmentation results obtained by different methods are noise sensitive, and the obtained outlines by these techniques are uneven excluding the proposed technique as shown in Fig. 2. From Fig. 2(g), this can be perceived that the proposed technique correctly segmented the lesion in spite of varying contrast and noise artifacts. The primary benefit of the proposed technique is that it is capable of managing the uncertain pixel values effectively and accurately; therefore, it helps to prevent the lesion boundary from linking false foregrounds in the segmentation results. Besides many advantages, proposed technique possesses the ability to perform segmentation of lesions even in noisy images and it is able to segment multiple lesions. The experiments performed on the CT images illustrate that the proposed technique based on SIFCM clustering and DRLSE outperform the other considered techniques for segmentation of renal lesions. The proposed technique is capable to segment lesions even in the presence of noise and blurry edges. This might serve as a second opinion to the doctors for correct segmentation of renal lesions. The performance of the proposed technique on different datasets is unidentified and may fluctuate significantly from the outcomes observed in this research work. Thus, in future, efforts will be made to investigate the performance of the suggested hybrid technique on diverse datasets gathered by distinct CT machines.

5 Conclusion

In this research paper, initially a SIFCM clustering method was employed which have shown remarkable results for segmentation of renal lesions as compared to the other state-of-the-art methods. To further improve the accuracy of the segmentation procedure a new hybrid technique based on spatial intuitionistic fuzzy c-means clustering and distance regularized level set was proposed for extraction of renal lesions from CT images. The technique assimilates the features of

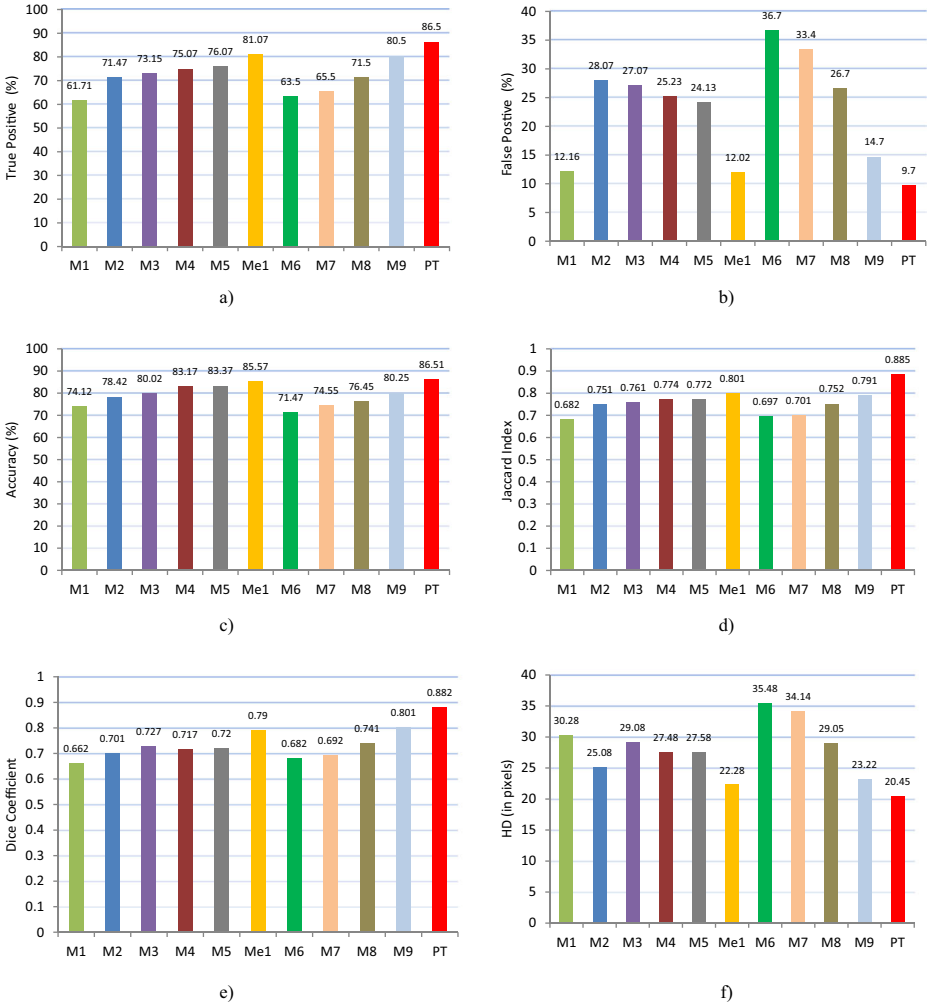

Fig. 3 Graph plots of the TP, FP, ACC, JI, DC and HD measurements for the segmentation of renal CT images processed with the different methods, whereas M1, M2, M3, M4, M5, M6, and M7 refers to the thresholding, region growing, FCM, SFCM, IFCM, ACWE,GAC,FCMLS and DRLSE method, respectively. Me1 represents Method 1, and PT represents proposed technique

SIFCM clustering method and level set, for extraction of renal lesions by considering intensity inhomogeneity and background image details which may vary. The quantitative and qualitative experimental results illustrated that the proposed technique attains better values for TP, TN, DC, HD, JI, and ACC as compared to the other considered techniques that endorse its applications in medical scenarios. Moreover, the proposed hybrid technique minimizes the manual interference which in turn reduces the execution time; it only requires a rough estimation of the region of interest given by SIFCM within the renal. This technique offers better segmentation outcomes and can be helpful for the medical community to delineate the renal lesion for further diagnosis. Further, this work can be extended by incorporating different shape and texture features for segmentation of lesions and a classifier can be developed which can differentiate between benign and malignant lesions using the features extracted from the segmentation outcomes.

Acknowledgements This research work has been funded by University Grant Commission (UGC), New Delhi, India. Additionally, the authors would like to thank Prof. Anupam Lal, Department of Radio-diagnosis, PGIMER, Chandigarh for his support in carrying out this research.

Compliance with ethical standards

Conflict of interest Authors have no conflict of interest

References

1. Ahmed MN, Yamany SM, Mohamed N, Farag AA, Moriarty T (2002) A modified fuzzy c-means algorithm for bias field estimation and segmentation of MRI data. IEEE Trans Med Imaging 21(3):193–199. https://doi.org/10.1109/42.996338
2. Archip N, Jolesz FA, Warfield SK (2007) A validation framework for brain tumor segmentation. Acad Radiol 14(10):1242–1251
3. Belongie S, Malik J, Puzicha J (2002) Shape matching and object recognition using shape contexts. IEEE Trans Pattern Anal Mach Intell 24(4):509–522
4. Bluth EI, Bush WH, Amis ES, Bigongiari LR, Choyke PL, Fritzsche PJ, Holder LE, Newhouse JH, Sandler CM, Segal AJ, Resnick MI (2000) Indeterminate renal masses: American College of Radiology. ACR Appropr Criteria Radiol 215:747–752
5. Cai W, Chen S, Zhang D (2007) Fast and robust fuzzy c-means clustering algorithms incorporating local information for image segmentation. Pattern Recogn 40(3):825–838. https://doi.org/10.1016/j.patcog.2006.07.011
6. Campbell SC, Novick AC, Belldegrun A, Blute ML, Chow GK, Derweesh IH, Faraday MM, Kaouk JH, Leveillee RJ, Matin SF, Russo P (2009) Guideline for management of the clinical T1 renal mass. J Urol 182(4):1271–1279. https://doi.org/10.1016/j.juro.2009.07.004
7. Chan TF, Vese LA (2001) Active contours without edges. IEEE Trans Image Process 10(2):266–277
8. Chen S, Zhang D (2004) Robust image segmentation using FCM with spatial constraints based on new kernel-induced distance measure. IEEE Trans Syst Man Cybern B (Cybern) 34(4):1907–1916. https://doi.org/10.1109/TSMCB.2004.831165
9. Choyke PL, Amis ES, Bigongiari LR, Bluth EI, Bush WH, Fritzsche P, Holder L, Newhouse JH, Sandler CM, Segal AJ, Resnick MI (2000) Renal cell carcinoma staging. American College of Radiology. ACR Appropr Criteria Radiol 215:721–725
10. Chuang KS, Tzeng HL, Chen S, Wu J, Chen TJ (2006) Fuzzy c-means clustering with spatial information for image segmentation. Comput Med Imaging Graph 30(1):9–15. https://doi.org/10.1016/j.compmedimag.2005.10.001
11. Fedkiw SO, Osher S (2002) Level set methods and dynamic implicit surfaces. Surfaces 44:77
12. Graves D, Pedrycz W (2010) Kernel-based fuzzy clustering and fuzzy clustering: a comparative experimental study. Fuzzy Sets Syst 161(4):522–543. https://doi.org/10.1016/j.fss.2009.10.021
13. Gupta D, Anand RS (2017) A hybrid edge-based segmentation approach for ultrasound medical images. Biomed Signal Process Control 1(31):116–126. https://doi.org/10.1016/j.bspc.2016.06.012
14. Kaur R, Juneja M (2016) A survey of different imaging modalities for renal cancer. Indian J Sci Technol 30(9):44–50. https://doi.org/10.17485/ijst/2016/v9i44/105067
15. Kaur R, Juneja M (2018) Comparison of different renal imaging modalities: an overview. In Progress in intelligent computing techniques: theory, practice, and applications (pp 47–57). Springer, Singapore. https://doi.org/10.1007/978-981-10-3373-5_4
16. Kaur R, Juneja M, Mandal AK (2018) A comprehensive review of denoising techniques for abdominal CT images. Multimed Tools Appl 1–36. https://doi.org/10.1007/s11042-017-5500-5
17. Kim DY, Park JW (2004) Computer-aided detection of kidney tumor on abdominal computed tomography scans. Acta Radiol 45(7):791–795
18. Lee HS, Hong H, Kim J (2017) Detection and segmentation of small renal masses in contrast-enhanced CT images using texture and context feature classification. In Biomedical Imaging (ISBI 2017), IEEE 14th International Symposium 18 (pp 583–586) https://doi.org/10.1109/ISBI.2017.7950588

19. Li C, Xu C, Gui C, Fox MD (2005) Level set evolution without re-initialization: a new variational formulation. In Computer Vision and Pattern Recognition. CVPR. IEEE Computer Society Conference 1 (pp 430–436) https://doi.org/10.1109/CVPR.2005.213
20. Li C, Xu C, Gui C, Fox MD (2010) Distance regularized level set evolution and its application to image segmentation. IEEE Trans Image Process 19(12):3243–3254. https://doi.org/10.1109/TIP.2010.2069690
21. Linguraru MG, Wang S, Shah F, Gautam R, Peterson J, Linehan WM, Summers RM (2011) Automated noninvasive classification of renal cancer on multiphase CT. Med Phys 38(10):5738–5746. https://doi.org/10.1118/1.3633898
22. Ljungberg B, Bensalah K, Bex A, Canfield S, Dabestani S, Hofmann F, Hora M, Kuczyk MA, Lam T, Marconi L, Merseburger AS (2013) Guidelines on renal cell carcinoma. Eur Assoc Urol 28
23. Osher S, Sethian JA (1988) Fronts propagating with curvature-dependent speed: algorithms based on Hamilton-Jacobi formulations. J Comput Phys 79(1):12–49. https://doi.org/10.1016/0021-9991(88)90002-2
24. Piao N, Kim JG, Park RH (2015) Segmentation of cysts in kidney and 3-D volume calculation from CT images. Int J Comput Graph Anim 5(1):1. https://doi.org/10.5121/ijcga.2015.5101
25. Siegel RL, Miller KD, Jemal A (2016) Cancer statistics 2016. CA Cancer J Clin 66(1):7–30. https://doi.org/10.3322/caac.21332
26. Smith RA, Andrews KS, Brooks D, Fedewa SA, Manassaram-Baptiste D, Saslow D, Brawley OW, Wender RC (2017) Cancer screening in the United States, 2017: a review of current American Cancer Society guidelines and current issues in cancer screening. CA Cancer J Clin 67(2):100–121. https://doi.org/10.3322/caac.21392
27. Summers RM, Agcaoili CM, McAuliffe MJ, Dalal SS, Yim PJ, Choyke PL, Walther MM, Linehan WM (2001) Helical CT of von Hippel-Lindau: semi-automated segmentation of renal lesions. In IEEE International Conference on Image Processing 2: (pp 293–296)https://doi.org/10.1109/ICIP.2001.958485
28. Thakur N, Juneja M (2018) Survey on segmentation and classification approaches of optic cup and optic disc for diagnosis of glaucoma. Biomed Signal Process Control 30(42):162–189. https://doi.org/10.1016/j.bspc.2018.01.014
29. Tolias YA, Panas SM (1998) On applying spatial constraints in fuzzy image clustering using a fuzzy rule-based system. IEEE Signal Process Lett 5(10):245–247. https://doi.org/10.1109/97.720555
30. Turner RM, Morgan TM, Jacobs BL (2017) Epidemiology of the small renal mass and the treatment disconnect phenomenon. Urol Clin 44(2):147–154. https://doi.org/10.1016/j.ucl.2016.12.001

Ravinder Kaur received her B.Tech. from SUSCET, PTU, Jalandhar (Punjab) in 2011, in Information Technology, and the M.E Degree from PEC University of Technology in 2013, in Computer Science and Engineering. She is awarded with Junior Research Fellow (JRF) award from university grant commission (UGC), New Delhi in 2015. She has published various papers in international journals and conferences. Presently, she is working as Senior Research Fellow (SRF) in the department of Computer Science and Engineering at University Institute of Engineering & Technology, Panjab University, Chandigarh, India. Her research interests include medical image processing.

Dr. Mamta Juneja received her B.Tech. and M.E. degree in Computer Science and Engineering. She obtained her Ph.D. degree in 2013 in the field of Image processing. She has been into the teaching profession since 2001 and has published more than 140 papers in refereed International Journals and conference proceedings with more than 667 citations in Google Scholar (with h-index of 11). She has served as reviewer for many reputed journals. Presently, she is working as Assistant Professor in the Department of CSE, University Institute of Engineering. & Technology, Panjab University, Chandigarh, India. She is working on various research projects funded by MHRD and DeITY. Her research interests include Medical image processing, Biometric Security and Data Hiding.

Dr. AK Mandal , MS, M.Ch is currently the Professor & Chairman of Department of Urology at the Postgraduate Institute of Medical Education and Research, Chandigarh, India (PGIMER). After completion of Medical schooling with Gold Medal in Surgery & Ophthalmology from the University of Calcutta he received MS (General Surgery) and M.Ch (Urology) from PGIMER, He has been teaching at the Department of Urology, PGIMER for the last 28 years. In 2005, he received Dr. Pinnamaneni Venkateshwara Rao Oration & Gold Medal of the Urological Society of India (USI). He is editorial board member of the several reputed journals and has co-authored over 200 scientific publications, review and conference proceedings articles. He is a member of several professional bodies which includes American Urological Association (AUA), Society De Internationale (SIU) and Urological Association of Asia (UAA). His areas of interest include Reconstructive Urology, Uro-Oncology, and Voiding Dysfunction. To recognize his contribution towards development of Urology in India, the Urological Society of India, during its Golden jubilee Year (2017) has chosen Dr. Mandal for the award of President's Gold Medal.